Heparin-binding VEGFR1 variants as long-acting VEGF inhibitors for treatment of intraocular neovascular disorders

Hong Xin[a], Nilima Biswas[a], Pin Li[a], Cuiling Zhong[a], Tamara C. Chan[b], Eric Nudleman[b], and Napoleone Ferrara[a,b,1]

[a]Department of Pathology, University of California San Diego, La Jolla, CA 92093; and [b]Department of Ophthalmology, University of California San Diego, La Jolla, CA 92093

Contributed by Napoleone Ferrara, April 20, 2021 (sent for review December 4, 2019; reviewed by Jayakrishna Ambati and Lois E. H. Smith)

Neovascularization is a key feature of ischemic retinal diseases and the wet form of age-related macular degeneration (AMD), all leading causes of severe vision loss. Vascular endothelial growth factor (VEGF) inhibitors have transformed the treatment of these disorders. Millions of patients have been treated with these drugs worldwide. However, in real-life clinical settings, many patients do not experience the same degree of benefit observed in clinical trials, in part because they receive fewer anti-VEGF injections. Therefore, there is an urgent need to discover and identify novel long-acting VEGF inhibitors. We hypothesized that binding to heparan-sulfate proteoglycans (HSPG) in the vitreous, and possibly other ocular structures, may be a strategy to promote intraocular retention, ultimately leading to a reduced burden of intravitreal injections. We designed a series of VEGF receptor 1 variants and identified some with strong heparin-binding characteristics and ability to bind to vitreous matrix. Our data indicate that some of our variants have longer duration and greater efficacy in animal models of intraocular neovascularization than current standard of care. Our study represents a systematic attempt to exploit the functional diversity associated with heparin affinity of a VEGF receptor.

angiogenesis | VEGF | age-related macular degeneration

The development of a neovascular supply or angiogenesis serves crucial homeostatic roles, since the blood vessels carry nutrients to tissues and organs and remove catabolic products (1). However, uncontrolled growth of blood vessels can promote or facilitate numerous disease processes, including tumors and intraocular vascular disorders (1). Although numerous angiogenic factors were initially identified and characterized (2), work performed in many laboratories has established vascular endothelial growth factor (VEGF) as a key regulator of normal and pathological angiogenesis as well as vascular permeability (3–5). Alternative exon splicing results in the generation of multiple isoforms that differ in their affinity for heparin, including $VEGF_{121}$, $VEGF_{165}$, and $VEGF_{189}$. $VEGF_{121}$ lacks significant heparin binding. While $VEGF_{165}$ has a single, exon-7-encoded, heparin-binding domain, $VEGF_{189}$ has two heparin-binding domains encoded respectively by exon-6 and exon-7 (6, 7). Much experimental evidence documents the key role of the heparin-binding VEGF isoforms in the establishment of biochemical gradients required for angiogenesis (8–10). VEGF is a member of a gene family that also includes PlGF, VEGF-B, VEGF-C, and VEGF-D. Three related receptor tyrosine kinases (RTKs) have been reported to bind VEGF ligands: VEGFR1 (11, 12), VEGFR2 (13), and VEGFR3 (14). VEGF binds both VEGFR1 and VEGFR2, while PlGF and VEGF-B interact selectively with VEGFR1. VEGFR3 and its two ligands, VEGF-C and VEGF-D, are primarily implicated in lymphangiogenesis (15, 16). Each member of this RTK class has seven immunoglobulin (Ig)-like domains in the extracellular portion (17). There is agreement that VEGFR2 is the main signaling receptor for VEGF (16), although VEGFR1 binds VEGF with substantially higher affinity than VEGFR2 (17).

VEGF inhibitors have become a standard of therapy in multiple tumors and have transformed the treatment of intraocular neovascular disorders such as the neovascular form of age-related macular degeneration (AMD), proliferative diabetic retinopathy, and retinal vein occlusion, which are leading causes of severe vision loss and legal blindness (3, 5, 18). Currently, three anti-VEGF drugs are widely used in the United States for ophthalmological indications: bevacizumab, ranibizumab, and aflibercept (3). Bevacizumab is a full-length IgG antibody targeting VEGF (19). Even though bevacizumab was not developed for ophthalmological indications, it is widely used off-label due to its low cost. Ranibizumab is an affinity-matured anti-VEGF Fab (20). Aflibercept is an IgG-Fc fusion protein (21), with elements from VEGFR1 and VEGFR2, that binds VEGF, PlGF, and VEGF-B (22). Importantly, after a 5-y treatment with ranibizumab or bevacizumab, about half of neovascular AMD patients had good vision, i.e., visual acuity 20/40 or better, an outcome that would not have been possible before anti-VEGF agents were available (23). However, in real-life clinical settings, many patients receive fewer anti-VEGF injections than in clinical trials, and it has been hypothesized that this correlates with less satisfactory visual outcomes (24). Therefore, there is a need to develop agents with longer duration after intraocular injection, thus reducing the frequency of injections, and a number of approaches to this end have been attempted (25, 26). Aflibercept (Eylea) was

Significance

Vascular endothelial growth factor (VEGF) inhibitors have transformed the treatment of intraocular vascular disorders. However, the burden of frequent intravitreal injections reduces patient compliance such that the impact in the "real world" is less than in clinical trials. Thus, there is a need to discover VEGF inhibitors than can be administered less frequently. We hypothesized that the ability to bind heparan-sulfate proteoglycans may be a strategy to promote intraocular retention and increase half-life. We designed a series of VEGF receptor 1 variants and identified some with strong heparin-binding characteristics that are more effective and durable in action in animal models of intraocular neovascularization than a standard of care like aflibercept. The work should fulfill an unmet medical need and advance therapy.

Author contributions: H.X., N.B., P.L., E.N., and N.F. designed research; H.X., N.B., P.L., C.Z., T.C.C., E.N., and N.F. performed research; H.X., N.B., P.L., and C.Z. analyzed data; and E.N. and N.F. wrote the paper.

Reviewers: J.A., University of Virginia; and L.E.H.S., Harvard Medical School.

Competing interest statement: The technology described in the manuscript has been licensed to a start-up company.

[1]To whom correspondence may be addressed. Email: nferrara@ucsd.edu.

This article contains supporting information online at https://www.pnas.org/lookup/suppl/doi:10.1073/pnas.1921252118/-/DCSupplemental.

Published May 18, 2021.

approved based on clinical trials showing that every 8-wk administration of the dose of 2 mg could match the efficacy of monthly ranibizumab (0.5 mg). However, despite the prediction that a switch to aflibercept would reduce the number of intravitreal injections, recent studies suggest that it is not the case (27). Another approach aiming to reduce frequency of injections is the use of high doses of brolucizumab, a recently Food and Drug Administration (FDA)-approved high-affinity single-chain variable fragments (scFV) targeting VEGF (28). However, an increased incidence of retinal vasculitis and intraocular inflammation that adversely affected vision has been observed in a subset of patients treated with brolucizumab (29). A refillable slow-release device system implanted in the vitreous that enables continuous delivery of ranibizumab has been developed (30). The phase II data reported are promising, but this approach requires surgery and complications such as bleeding have been noted (30). Therefore, there is still an unmet medical need for intravitreal anti-VEGF agents with improved half-life.

In 1996, in the course of structure–function studies aiming to identify VEGF-binding elements in VEGFR1, we found that deletion of Ig-like domain (D) 2, but not of other Ds, abolished VEGF or PIGF binding (31). Replacing D2 of VEGFR3 with D2 of VEGFR1 conferred on VEGFR3 the ligand specificity of VEGFR1 and abolished the ability of the mutant VEGFR3 to interact with VEGF-C (31). Subsequent studies documented the interaction between D2 and VEGF (or PlGF) by X-ray crystallography (32–34). However, D3 was important for optimal VEGF binding (31, 32). These initial studies led to the design of a construct comprising the first three lg-like Ds of VEGFR1, fused to an Fc-lgG (Flt-1-3-IgG) (31). Flt-1-3-lgG showed a potent ability to neutralize VEGF in vitro and in several in vivo models of physiological and pathological angiogenesis (35–40). However, the half-life of this molecule following systemic administration was relatively short due to the presence of clusters of basic residues in D3, which resulted in binding to heparan-sulfate proteoglycans (HSPG) and sequestration in the extracellular matrix of various tissues.

In 2002, Holash et al. (22) described an IgG fusion construct comprising VEGFR1 D2 and VEGFR2 D3, which has much lower heparin affinity than VEGFR1 D3. This molecule, known today as aflibercept, ziv-aflibercept, or Eylea, was reported to have a significantly longer systemic half-life than Flt(1-3-lgG) (22). These pharmacokinetic characteristics, combined with high binding affinity for VEGF and the ability to bind PlGF and VEGF-B, led to the prediction that aflibercept would be a more effective antitumor agent than other VEGF inhibitors (22, 41). However, aflibercept has gained FDA approval only for second line treatment of colorectal cancer, while bevacizumab and the anti-VEGFR2 antibody ramucirumab received several FDA approvals in multiple cancer types (3, 5), suggesting that the above-mentioned characteristics did not provide a therapeutic advantage. Clearly, aflibercept has had its major clinical impact as an intravitreal treatment for ocular vascular disorders.

We hypothesized that heparin-binding mediated by D3 (or other Ig-like domain) of VEGFR1 (12), while a disadvantage for systemic administration, might confer significant advantages for intravitreal and potentially other local administration.

Results

To identify more effective and longer-lasting VEGF inhibitors for intraocular use, we sought to exploit the diversity of heparin binding in VEGFR1 Ds. To this end, we designed eight VEGFR1-Fc fusion constructs having differential heparin binding, thus providing a spectrum of HPSG affinity. Fig. 1 illustrates the domain structure of these proteins and highlights heparin-binding domains. All proteins include D2, the key determinant of ligand specificity (31). Two constructs (V1233 and V233) have a duplicated D3. The domain structure of aflibercept is also shown.

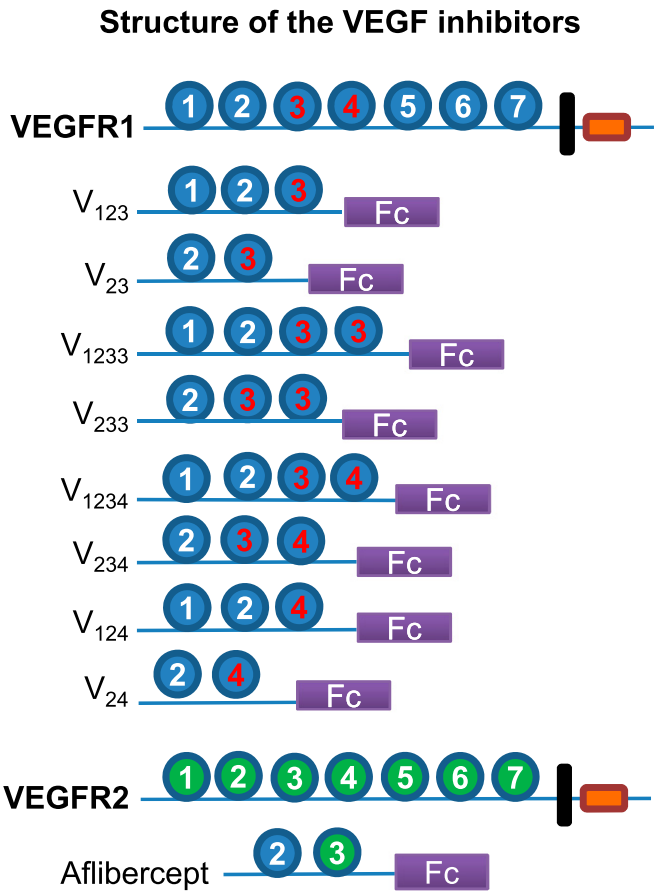

Fig. 1. Immunoglobulin (Ig)-like domain (D) organization of VEGFR1 and of the Fc fusion constructs designed in our study. Red label denotes heparin-binding domain. D2 is an indispensable binding element for VEGF and PlGF, responsible for ligand specificity (31). D3 plays an important role in binding affinity and stability (31, 32, 34). D3 of VEGFR1, but not D3 of VEGFR2, is a major heparin-binding site. V23 and aflibercept (Eylea) differ only in D3, which is from VEGFR2 in aflibercept. D4 is also a heparin-binding site, implicated in receptor dimerization and homotypic interactions (34). Each construct is shown as a monomer for simplicity, but the recombinant proteins are dimers due to the forced dimerization imposed by the Fc.

In initial experiments, we noted that the expression levels of several of our constructs were low; V1234, V1233, V234, and V124 were detectable at low levels in the conditioned media. Interestingly, earlier studies had shown that VEGF isoforms with high affinity for heparin ($VEGF_{189}$ or $VEGF_{206}$) are almost undetectable in the conditioned media of transfected cells, being largely bound to the cells surface or the extracellular matrix (10, 42). However, they could be released in a soluble form by the addition of heparin or heparinase, indicating that the binding site consisted of HSPG (10, 42). Thus, we sought to determine whether the addition of heparin may affect the release of our recombinant VEGFR1 fusion proteins. Indeed, adding heparin to the media of transfected cells resulted in dose-dependent increases in the concentrations of recombinant proteins, with a maximal effect at the concentration of 100 μg/mL. Depending on the construct, the fold increases at this heparin concentration ranged between 1.2 and 10.6 relative to no addition. Therefore, we routinely added 100 μg/mL heparin to the media.

We initially attempted to purify the recombinant proteins simply by conventional protein A (PA) affinity chromatography. However, this method yielded a major band of the expected mass and numerous other minor bands, likely reflecting the interaction

of the strongly basic, heparin-binding, recombinant proteins with host cell-derived HSPGs and other anionic molecules. We therefore developed a protocol that removed such impurities, as described in *Materials and Methods*. A wash at high pH (9.2) in the presence of 1.2 M NaCl, while the protein is bound to PA, resulted in release of numerous contaminants. The next step, anion exchange chromatography, was very effective at removing the bulk of contaminants and aggregates, while the purified protein was in the flow through. The LPS levels in the final purified preparations were <0.1 EU/mg (range 0.02 to 0.08), a very low level compatible with preclinical studies (43). As shown in Fig. 2*A*, the purity of our recombinant proteins was >95%, as assessed by silver-stained sodium dodecyl sulphate–polyacrylamidegel electrophoresis (SDS/PAGE), and was similar to that of the FDA-approved drug Eylea. Fig. 2*B* shows analytical size exclusion chromatography (SEC) profiles of the three most promising candidates, V23, V1233, and V233, next to Eylea. Similar to Eylea, the three proteins eluted as a single peak at the expected retention time, without significant aggregation.

We tested the recombinant proteins for their ability to inhibit mitogenesis induced by $VEGF_{165}$ (10 ng/mL) in bovine choroidal endothelial cells (BCECs). As illustrated in Fig. 3, they had inhibitory effects, with the half maximal inhibitory concentration (IC_{50}) values in the range of ∼1 nM, except for V124 and V24, which were less potent. We also documented their ability to inhibit BCEC mitogenesis stimulated by $VEGF_{121}$ (*SI Appendix*, Fig. S1). Interestingly, Eylea in nearly all experiments (>10) was potent, being active at low concentrations, with IC_{50} of ∼1 nM, but inhibited no more than ∼80% of VEGF-stimulated BCEC proliferation even at the highest concentrations tested. Similar results were obtained using HUVEC proliferation assays (*SI Appendix*, Fig. S2). In contrast, our VEGFR1 constructs (except V124 and V24) completely blocked VEGF-induced proliferation. The ability to detect such differences likely reflects the relatively high dynamic range of our BCEC proliferation assay in response to VEGF stimulation (approximately fourfold increase). In addition, we compared V1233, V233, and aflibercept in a recently developed short-term (6 h) cell-based assay kit (Promega) that measures VEGF stimulation in HEK-293 cells engineered to express VEGFR2, using luciferase as a readout. In this assay, the three proteins showed very similar inhibitory potency (*SI Appendix*, Fig. S3).

Although the significance of the less than complete inhibition of BCEC proliferation by Eylea remains to be fully investigated, it is not inconceivable that VEGFR1 D3 provides a better interactive surface than D3 from VEGFR2, especially considering that VEGFR1 binds VEGF significantly more effectively than VEGFR2 (44, 45). To test this hypothesis, we performed a comparison of Protein Data Bank files of the VEGFR1/VEGF complex (5T89) (34) and VEGFR2/VEGF complex (3V2A) (46) and superimposed D2 to D3 from each receptor. This analysis supports our hypothesis. For example, Arg280 in VEGFR1 D3 interacts with the sidechain of VEGF Phe36, whereas VEGFR2 has an Asp there. Likewise, in VEGFR1 both Arg261 and Asn290 interact with VEGF Glu64; in VEGFR2, the Arg261 is replaced by Gly and hence in VEGFR2 only the Lys replacing Asn290 can interact with VEGF Glu64. *SI Appendix*, Fig. S4 illustrates the VEGFR1 residues that can potentially interact with VEGF and that differ between VEGFR1 and VEGFR2.

To further define therapeutically relevant interactions, we sought to assess whether our recombinant proteins bind bovine vitreous in vitro. As illustrated in Fig. 4, while Eylea, control IgG, or Avastin had little or no binding, our proteins showed significant binding. The strongest binders were V1233, V233, and V1234, followed by V123. V23 had intermediate binding characteristics, between Eylea (or control IgG) and V1233.

We tested our recombinant proteins in the mouse laser-induced choroidal neovascularization (CNV) model and compared them to control IgG or Eylea. An extensive literature documents the ability of anti-VEGF agents to suppress neovascularization in this model (47–49). We initially chose to test relatively low doses for proof-of-concept studies, being best suited to reveal potency and

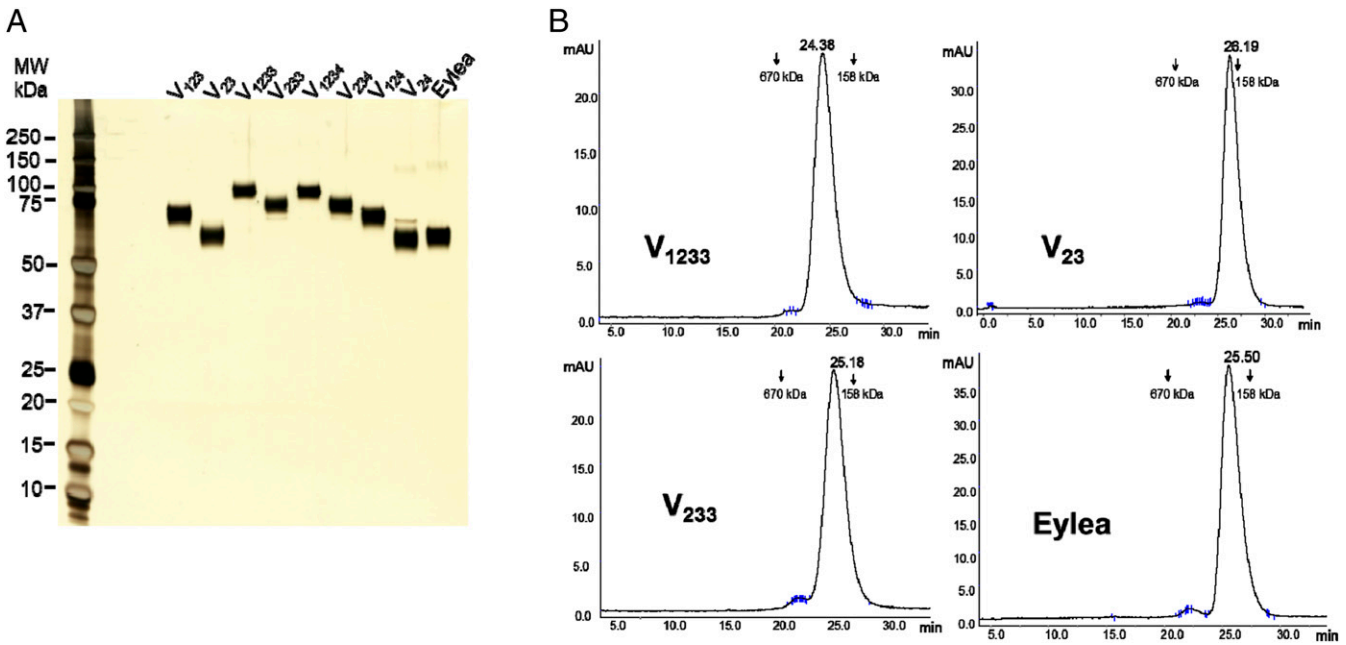

Fig. 2. Characterization of purified recombinant proteins. (*A*) Silver-stained SDS/PAGE (4 to 20% Tris) of our purified recombinant fusion proteins and Eylea. A total of 200 ng of each protein was subjected to electrophoresis under reducing conditions. Staining was performed by SilverQuest Silver Staining Kit (Invitrogen). (*B*) Analytical SEC of V23, V233, V1233, and Eylea, 25 μg of each. The *y* axis represents intensity of absorbance (A_{280}) in milli-absorbance units, and the *x* axis represents elution time in minutes.

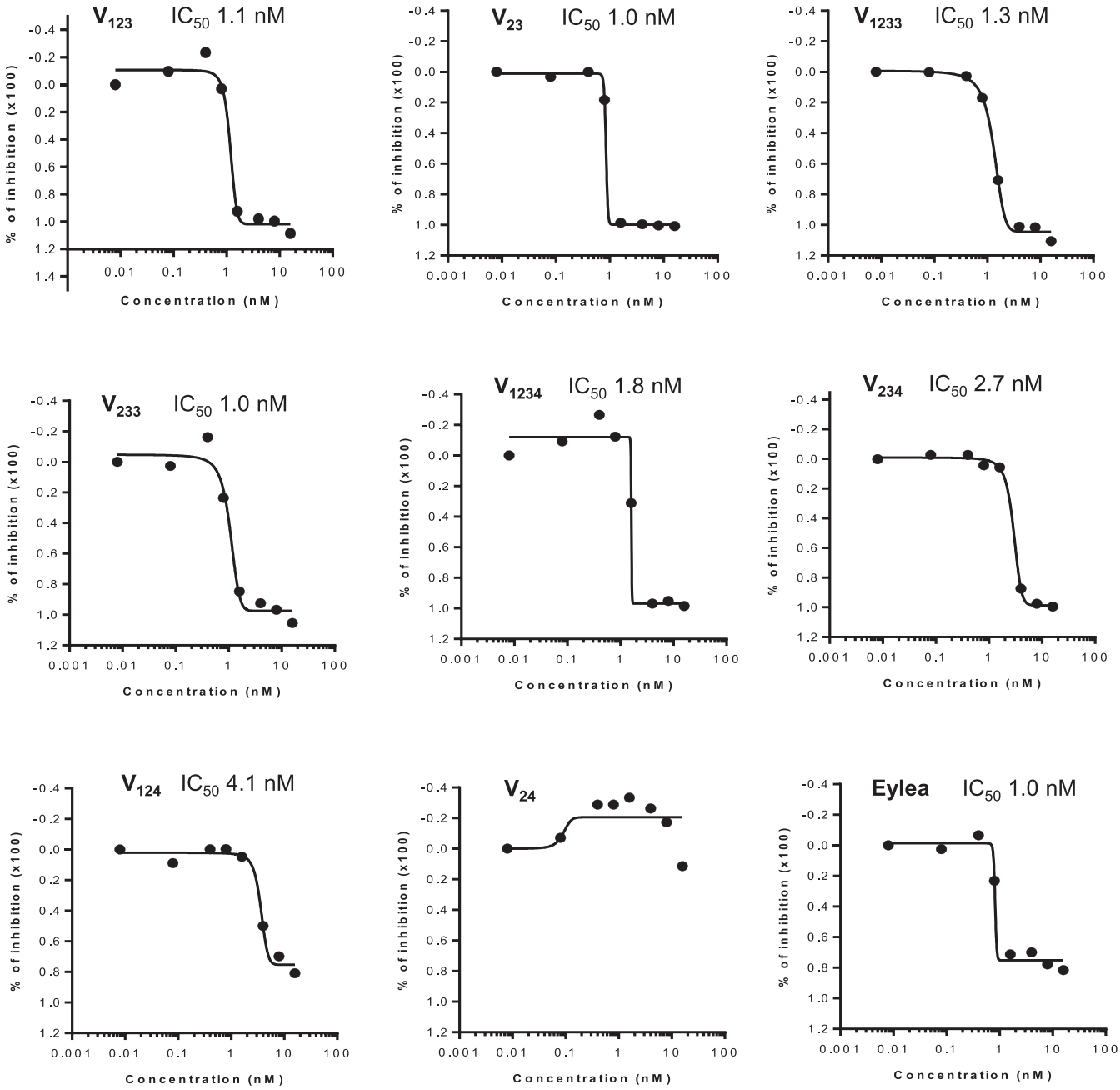

Fig. 3. IC_{50} values of the inhibitors. Bovine choroidal ECs were maintained as described in *Materials and Methods*. For assays, cells are plated at low density. Inhibitors were then added at various concentrations as indicated. $VEGF_{165}$ was added at the final concentration of 10 ng/mL. Cell densities were evaluated after 5 d. IC_{50} values were calculated using GraphPad Prism 5 (GraphPad Software). Data shown are based on two independent experiments obtained with highly purified proteins and are consistent with numerous previous assays.

durability differences among the various proteins. Also, it has been reported that intravitreal administration of high doses of antibodies of the IgG1 isotype may have off-target angioinhibitory effects, mediated by Fc signaling through FcgRI and c-Cbl, leading to impaired macrophage migration (50). These effects might potentially confound the interpretation of the data. The doses that we employed are efficacious and at the same time should avoid such off-target effects. Initially, each protein was injected intravitreally at the dose of 2.5 μg 1 d before laser treatment. Eylea was tested also at 25 μg. As illustrated in Fig. 5*A*, Eylea resulted in an ∼30% inhibition at the dose of 2.5 μg and ∼50% inhibition at the dose of 25 μg. These findings are largely consistent with the published literature. For example, Saishin et al. reported that the intravitreal injection of ∼5 μg of aflibercept resulted in ∼30% inhibition of the CNV area in the mouse (48). Indeed, the dose of 40 μg is commonly used to achieve maximal inhibitory effects of aflibercept in the mouse CNV model (51). An unexpected finding was the greater potency of some of our constructs: V123, V23, V1233, and V233. Administering 2.5 μg of these proteins, 1 d before the injury, matched or even exceeded the level of inhibition achieved with 25 μg of Eylea. However, none of the constructs that included D4 demonstrated significant CNV inhibition (Fig. 5*A*).

To determine whether heparin binding may translate in durable therapeutic effects following a single administration, V1233, Eylea, or control IgG, were injected intravitreally (2.5 μg) 1, 7, or 14 d before the laser-induced injury. As shown in Fig. 5*B*, Eylea resulted

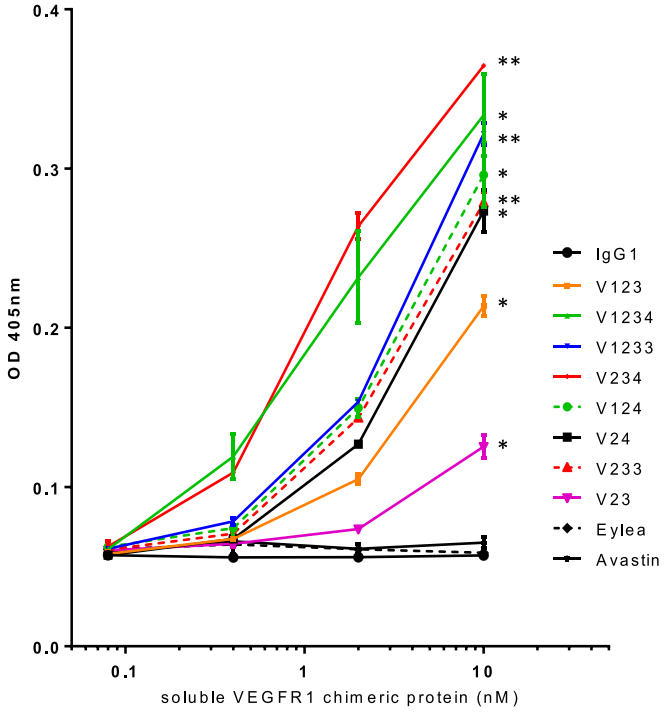

Fig. 4. In vitro binding of Fc-containing proteins to bovine vitreous. Two independent experiments were performed in duplicate wells as described in *Materials and Methods*. Note the concentration-dependent binding, except for Eylea, Avastin, and control IgG. The 10-nM groups were compared to the control IgG group by Student's *t* test for significance. $^{**}P < 0.01$, $^{*}P < 0.05$.

in a significant inhibition only when administered 1 d before the injury. In contrast, V1233 resulted in a significant inhibition also when administered 7 or 14 d prior to the injury. In a subsequent study, we compared equimolar amounts of Eylea, V23, V1233, and V233, (4.8 μg of Eylea and V23, 6.3 μg of V233, and 7.2 μg of V1233), administered 14 d prior to the injury. Fig. 5*C* shows that, at the dose tested, Eylea had very little effect on CNV. In contrast, V23, V1233, and V233 resulted in a significant CNV inhibition. A prediction of our hypothesis is that inhibitors with strong heparin-binding characteristics will have lower systemic exposure compared to Eylea. We injected intravitreally, in both eyes, equimolar amounts of Eylea, V23, V233, or V1233 and measured human Fc serum levels at different time points up to 21 d after intravitreal administration, as shown in Fig. 5*D*. Eylea administration resulted in the highest serum levels throughout the experiment. V23, which has a single heparin-binding domain, resulted in lower serum levels than Eylea, but trended higher than V1233 or V233.

Finally, we compared multiple doses of V1233 and Eylea in the oxygen-induced retinopathy (OIR) model. Eyes were injected at postnatal day 7 (P7), prior to placement in the hyperoxic chamber, and analyzed at P12 and P17 for the extent of vasoobliteration (VO) and neovascularization (Fig. 6). In agreement with the findings in the CNV model, V1233 was more potent than Eylea at inhibiting neovascularization (Fig. 6 *A*–*C*). Importantly, whereas Eylea at a concentration of 2.5 μg failed to inhibit NV, the molar equivalent of V1233 at a concentration of 3.8 μg significantly reduced NV (Fig. 6*C*). In addition, although all eyes had a similar degree of VO at P12 (Fig. 6*D*), a significant reduction in VO was found in eyes treated with 3.8 μg of V1233 but not with Eylea 2.5 μg (Fig. 6*E*).

Discussion

Interaction of D3 with the HPSG has been long considered a limitation of VEGFR1-based anti-VEGF strategies due to sequestration in various tissues, resulting in reduced systemic half-life. To overcome this issue, Holash et al. replaced VEGFR1 D3 with VEGFR2 D3 (22). To the same aim, Lee et al. more recently introduced a glycosylation site in VEGFR1 D3, effectively neutralizing positive charges and thus eliminating D3-mediated HSPG binding (52). In both cases, systemic half-life was increased relative to the original VEGFR1 construct (22, 52).

We designed a series of VEGFR1-Fc fusion constructs having differential abilities to interact with HSPGs. Our premise was that heparin binding, mediated by VEGFR1 D3 (or another Ig-like D such as D4) (53), while a disadvantage for systemic treatment, might confer unique advantages on a VEGF inhibitor to be used for intravitreal administration, since 1) it should anchor the inhibitors to HPSGs or other anionic molecules in the vitreous or other structure in the eye, thus increasing its half-life; and 2) such an inhibitor in principle does not need to be uniformly distributed or to deeply penetrate into the eye structures in order to effectively bind and block VEGF. Indeed, a variety of studies has shown that VEGF can diffuse to a considerable distance from its production site in response to biochemical gradients determined by HPSG or receptor distributions in the vasculature or in other sites (9, 10, 54). For example, although VEGF is produced by tumor cells, even at a significant distance from the vasculature, it diffuses and accumulates in the blood vessels by virtue of its high affinity for the VEGF receptors (55–57). Therefore, HPSG-bound VEGFR1 variants are expected to generate strong gradients, capable of attracting and neutralizing VEGF.

Given the challenges in obtaining accurate affinity measurements using sensor platforms such as surface plasmon resonance (SPR) with very tight binders (kDa <100 PM) (58), the conflicting data regarding the affinity of aflibercept versus other VEGF inhibitors (22, 59) and the poor correlation between binding affinity and therapeutic potency/efficacy among neutralizing antibodies to VEGF and other targets (60, 61), we chose to focus on biological IC_{50} data, being more physiologically relevant. As illustrated in Fig. 3, our recombinant proteins had inhibitory effects, with IC_{50} values in the range of ~1 nM, except V124 and V24, which were significantly less potent.

We were able to document that these proteins bind to bovine vitreous. The strongest binders were V1233, V1234, followed by V123. V23 had significant but lower vitreous binding. Control IgG, Eylea, and Avastin, had minimal binding. However, it should be noted that there are reported changes in HPSG composition in human vitreous humor with aging that might affect interaction with these proteins (62, 63).

An unexpected finding of our study was the potency of some of our constructs: V123, V23, V1233, and V233. Administering 2.5 μg of these constructs 1 d before the injury matched or even exceeded the level of inhibition achieved with 25 μg of Eylea. The finding that V1233, but not Eylea, has a significant effect in preventing CNV when administered 7 d or 14 d before the injury, documents the durability of the effects and the potential therapeutic value.

Also, we found that intravitreal injection of our heparin-binding proteins results in much lower systemic levels than Eylea. This property might be particularly useful, for example, for the treatment of retinopathy of prematurity, since it has been reported that treatment with anti-VEGF agents with significant systemic exposure might have detrimental neurodevelopmental effects (64, 65). Consistent with our results of systemic exposure following intravitreal injection of Eylea, fellow eye effects in OIR have been reported (62). While the present, short-term experiments do not discriminate between one and two heparin-binding domains, based on earlier work on VEGF isoforms, one might expect that, initially, the more diffusible V23 might be equally effective, but on a longer-term basis, the stronger interaction with the matrix of V233 or V1233 might prove advantageous (8).

Interestingly, none of the constructs containing D4 (V1234, V234, V124, and V24) resulted in marked inhibition in vivo (at least at the dose tested), despite the fact that these molecules

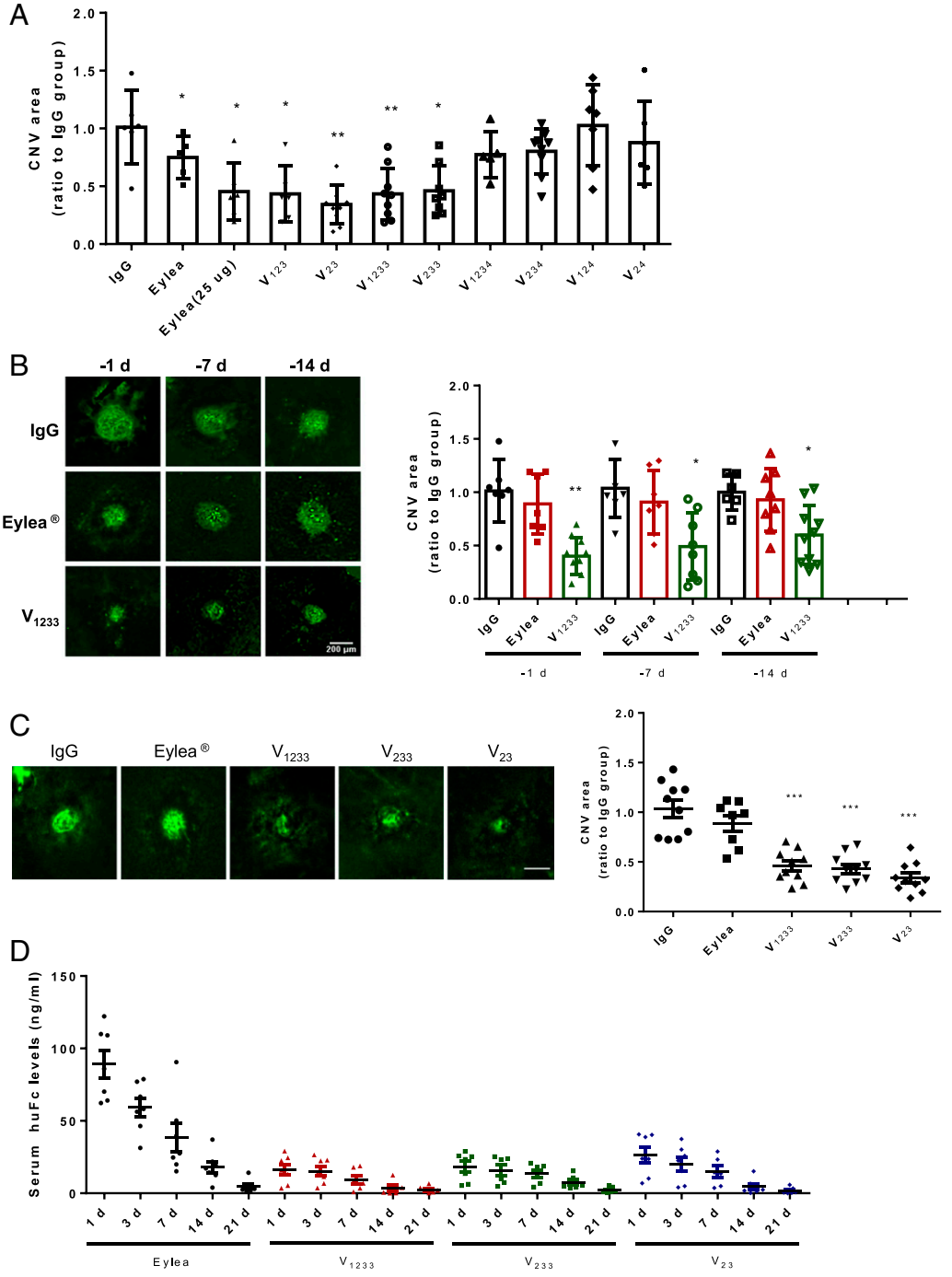

Fig. 5. Effects of control IgG, Eylea, or VEGFR1 Fc fusion proteins on laser-induced CNV in adult mice. (*A*) Each protein was injected intravitreally in the mouse at the dose of 2.5 μg 1 d before laser treatment. Eylea was tested also at 25 μg. Asterisks denote significant differences (Student's *t* test) compared to the appropriate IgG control groups (**$P < 0.01$, *$P < 0.05$). Data are based on three independent experiments with at least five mice per group. Note that the efficacy of Eylea is in line with the published literature in the same model. (*B*) Effect of the time of injection prior to injury on CNV area. Eylea at the dose of 2.5 μg had a significant reduction only when injected at day −1. In contrast, V1233 at the same dose significantly reduced CNV area even when injected 7 or 14 d prior to the injection. *Left* shows representative CD31 immunofluorescence images. Asterisks denote significant differences (Student's *t* test) compared to the appropriate IgG control groups (**$P < 0.01$, *$P < 0.05$). $n = 5$. Similar results were obtained in two independent experiments. (*C*) V23, V233, and V1233, tested at equimolar doses (4.8 μg of Eylea and V23, 6.3 μg of V233, and 7.2 μg of V1233), show greater efficacy compared to Eylea. All agents were administered 14 d prior to the laser treatment. Seven days later, eyes were harvested, and data were analyzed. Asterisks denote significant differences (Student's *t* test) compared to the appropriate IgG control groups (**$P < 0.01$, *$P < 0.05$). (*D*) Serum levels of Eylea, V23, V233, or V1233 in mice at different time points after intravitreal injection. Each molecule was injected in both eyes in equimolar amounts: 2.4 μg of Eylea and V23, 3.15 μg of V233, and 3.6 μg of V1233. After 1, 3, 7, 14, and 21 d, peripheral blood was collected from the tail vein. Human Fc levels were measured by ELISA. Values shown are means ± SEM. *$P < 0.05$, **$P < 0.01$, ***$P < 0.001$. $n = 8$ per point.

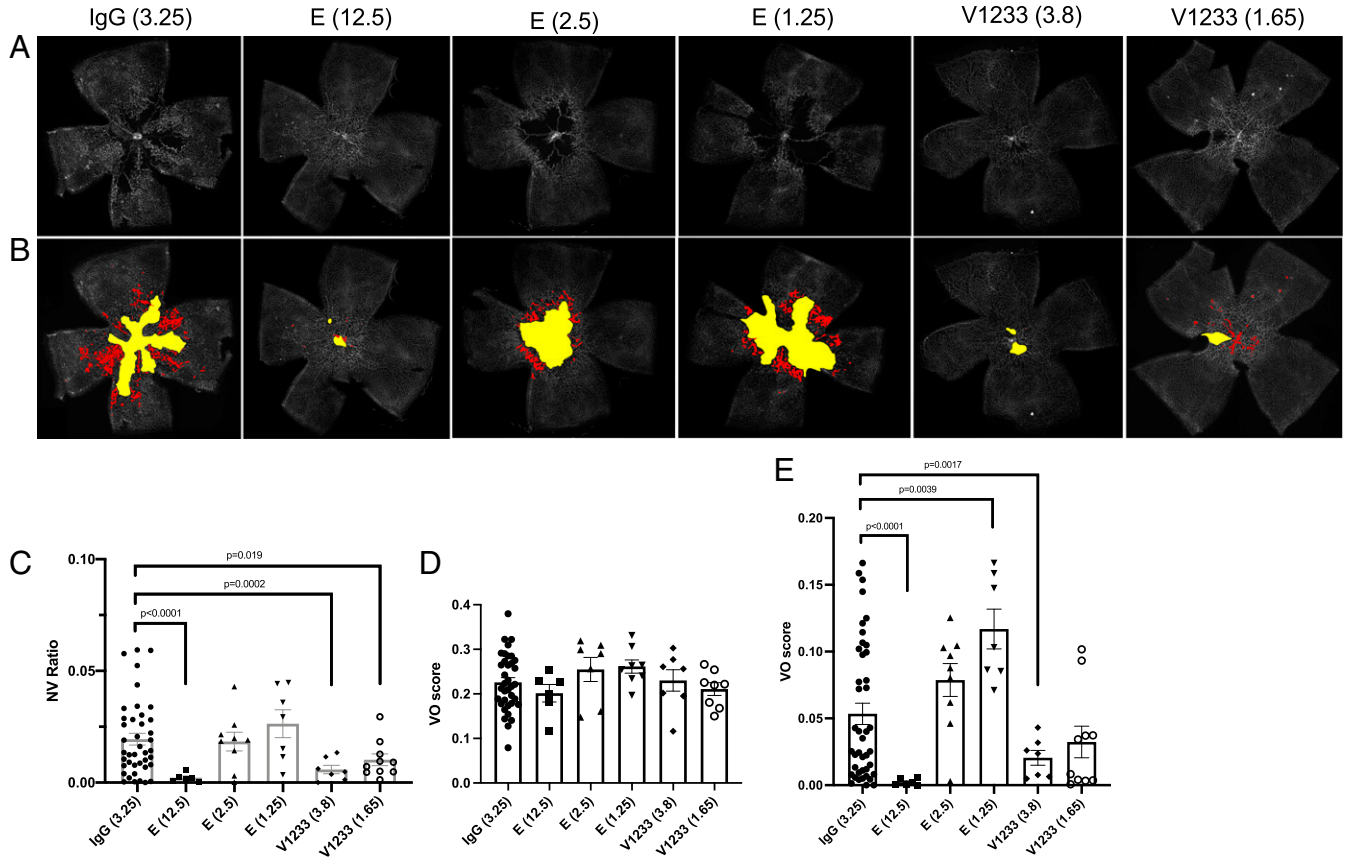

Fig. 6. Intravitreal injections of V1233 inhibit neovascularization in the OIR model. (*A*) Intravitreal injections were performed at P7 in C57BL/6J mice using aflibercept (Eylea), V1233, and control (IgG). A volume of 0.5 μL aflibercept (Eylea) (E) at a dose of 12.5, 2.5, or 1.25 μg versus control IgG at a dose of 3.25 μg injected into the fellow eyes. Littermates were injected with V1233 (3.8 μg or 1.65 μg) and control. The concentrations of IgG control, aflibercept 2.5 μg, and V1233 3.8 μg were equimolar. Animals were then exposed to 75% oxygen from P7 to P12 followed by return to room air. At P17, the animals were perfusion fixed, and the eyes were enucleated, dissected, stained with lectin from Bandeiraea simplicifolia (BSL)-fluorescein isothiocyanate (FITC), and flat mounted. (*B*) Vasoobliteration and neovascularization were analyzed using automated software as described by Xiao et al. (72). The vasoobliterative areas are shown in yellow, and neovascular tufts are shown in red. (*C*) Quantification of neovascularization shows a significant reduction ($P < 0.05$ *t* test with Welch's correction) in neovascularization relative to control with V1233 (3.8 and 1.65 μg) or high-dose aflibercept (12.5 μg), but not with aflibercept at 2.5 or 1.25 μg. (*D*) Quantification of vasoobliteration at P12 and (*E*) P17. No significant difference in VO was seen at P12 in any condition. At P17, however, a significant reduction in VO was seen with V1233 3.8 μg and high-dose aflibercept (12.5 μg), but neither with V1233 1.65 μg nor aflibercept 2.5 or 1.25 μg.

(with the exception of V24) demonstrated an ability to inhibit VEGF-stimulated mitogenesis in vitro. However, all of these constructs demonstrated a propensity to form oligomers or aggregates, as assessed by SDS/PAGE under nonreducing conditions and size exclusion chromatography, while V23, V123, V233, and V1233 showed the expected molecular mass (Fig. 2 *A* and *B*). Although earlier work (66) identified D4 (together with D7) as a requirement for VEGFR1 dimerization, such an effect has been known to be ligand dependent. Crystal structure studies revealed a loop in D4 responsible for such homotypic interactions (34). It is conceivable that high concentrations and/or the forced dimerization imposed by the Fc construct may result in ligand-independent interactions, resulting in aggregation. In any event, aggregates are not desirable pharmaceuticals, given the possibility of inflammation and immunogenicity (67, 68). Importantly, the lack of significant efficacy of our D4-including proteins argues against the possibility that a contaminant may be responsible for the observed efficacy, since all proteins were purified by the same methodology and have strong heparin-binding properties.

In conclusion, aflibercept was designed to eliminate heparin-binding characteristics in order to improve systemic half-life for oncological indications. The constructs described in the present study are instead designed to promote binding and retention in the vitreous and potentially other structures in the eye to ensure more sustained and therapeutically relevant interactions.

Materials and Methods

Plasmid Construction. For construction of VEGFR-Fc expression plasmids, the nucleic acid fragments encoding the signal peptide and a combination of extracellular Ig-like domains D1 to D4 of VEGRF1 (31) (Gene ID: 2321) were synthesized by GenScript USA, Inc. The following constructs were done: V123, D1, D2, and D3; V23, D2, and D3; V1233, D1, D2, D3, and D3; V233, D2, D3, and D3; V1234, D1, D2, D3, and D4; V234, D2, D3, and D4; V124, D1, D2, and D4; and V24, D2, and D4. The synthesized fragments were inserted into pFUSE-hIgG1-Fc1 vector (InvivoGen, #pfuse-hg1fc1) at *Eco*RI and *Bgl*II sites, generating the plasmids containing the various VEGFR1 extracellular domains (ECDs). Then, using PrimeSTAR Mutagenesis Basal Kit (Takara, R046A), the interval amino acids R and S (*Bgl*II site) between the ECDs and the Fc fragment were removed, generating the plasmids expressing the fusion proteins of VEGFR1 ECDs with a 227-amino acid human IgG1-Fc.

Transfection and Conditioned Media Preparation. The Expi293 expression system (Life Technologies, A14524) was used to generate the conditioned media for purification, according to the manufacturer's instructions. In brief, Expi293F cells (Thermo Fisher) were suspension cultured in Expi293 expression medium at 37 °C in a humidified atmosphere with 8% CO_2. When the cell density reached 2.5 million/mL, plasmid DNA and ExpiFectamine 293 reagent were mixed, incubated for 5 min, and added to the cells. The final

concentration of the DNA and transfected reagent was 1 μg and 2.7 μL per milliliter, respectively. Five hours after transfection, 100 μg/mL porcine heparin (Sigma, H3149) and protease inhibitor mixture, 1:400 (Sigma, P1860), were added to the cells. Sixteen hours after transfection, enhancer reagents 1 and 2 were added. Ninety-six hours after transfection, conditioned media were harvested. Aliquots were tested for Fc fusion protein concentrations using a human Fc ELISA Kit (Syd Labs, EK000095-HUFC-2) according to the manufacturer's instructions. Protease inhibitors were added (1:500) to the bulk, which was stored at −80 °C until further use.

Endothelial Cell Proliferation Assays. Endothelial cell (EC) proliferation assays were performed essentially as previously described (69–71). Primary BCECs (passage <10) (VEC Technologies, Cat. No. BCME-4) were trypsinized, resuspended, and seeded in 96-well plates (no coating) in low glucose Dulbecco's Modified Eagle Medium (DMEM) supplemented with 10% bovine calf serum, 2 mM glutamine, and antibiotics, at a density of 1,000 cells per well in a 200-μL volume. rhVEGF$_{165}$ (R&D Systems, Cat. No. 293-VE-010) or rhVEGF$_{121}$ (R&D Systems, Cat. No. 4644-VS010) was added at a concentration of 10 ng/mL. Aflibercept (Eylea) was purchased from a pharmacy. The inhibitors were added to cells at various concentrations, as indicated in the figures, before adding the ligands. After 5 or 6 d, cells were incubated with cell viability reagent (Advanced BioReagents, K020) for 4 h. Fluorescence was measured at 530-nm excitation wavelength and 590-nm emission wavelength.

Primary HUVECs from pooled donors (Lonza, Cat. No. C2519A) at a passage of less than 9 were cultured on 0.1% gelatin-coated plates in endothelial cell growth media EGM-2 (Lonza). Cells were maintained at 37 °C in a humidified atmosphere with 5% CO_2. To measure cell proliferation, 1,800 HUVECs suspended in 200 μL of endothelial basal growth media EBM-2 (Lonza) containing 0.5% fetal bovine serum, were seeded in 96-well plates. Four hours later, recombinant Fc fusion proteins and Eylea at concentrations of 10, 20, 50, 250, 500, 1,000, and 2,000 ng/mL were added to cells along with 10 ng/mL of VEGF$_{165}$. Cells were cultured for 3 d, and cell viability was determined by cell viability reagent following the manufacturer's instructions.

Data Availability. All study data are included in the article and/or supporting information.

ACKNOWLEDGMENTS. We thank Dr. Leonard G. Presta for modeling the differential interaction of VEGF-A with Ig-like domain 3 of VEGFR1 versus VEGFR2. We thank Dr. Karen Messer for help and advice in statistical analyses. This work was supported by NIH grant EY031345.

1. J. Folkman, M. Klagsbrun, Angiogenic factors. *Science* **235**, 442–447 (1987).
2. M. Klagsbrun, P. A. D'Amore, Regulators of angiogenesis. *Annu. Rev. Physiol.* **53**, 217–239 (1991).
3. N. Ferrara, A. P. Adamis, Ten years of anti-vascular endothelial growth factor therapy. *Nat. Rev. Drug Discov.* **15**, 385–403 (2016).
4. N. Ferrara, H. P. Gerber, J. LeCouter, The biology of VEGF and its receptors. *Nat. Med.* **9**, 669–676 (2003).
5. R. S. Apte, D. S. Chen, N. Ferrara, VEGF in signaling and disease: Beyond discovery and development. *Cell* **176**, 1248–1264 (2019).
6. K. A. Houck *et al*., The vascular endothelial growth factor family: Identification of a fourth molecular species and characterization of alternative splicing of RNA. *Mol. Endocrinol.* **5**, 1806–1814 (1991).
7. E. Tischer *et al*., The human gene for vascular endothelial growth factor. Multiple protein forms are encoded through alternative exon splicing. *J. Biol. Chem.* **266**, 11947–11954 (1991).
8. J. E. Park, G.-A. Keller, N. Ferrara, The vascular endothelial growth factor (VEGF) isoforms: Differential deposition into the subepithelial extracellular matrix and bioactivity of extracellular matrix-bound VEGF. *Mol. Biol. Cell* **4**, 1317–1326 (1993).
9. C. Ruhrberg *et al*., Spatially restricted patterning cues provided by heparin-binding VEGF-A control blood vessel branching morphogenesis. *Genes Dev.* **16**, 2684–2698 (2002).
10. N. Ferrara, Binding to the extracellular matrix and proteolytic processing: Two key mechanisms regulating vascular endothelial growth factor action. *Mol. Biol. Cell* **21**, 687–690 (2010).
11. M. Shibuya *et al*., Nucleotide sequence and expression of a novel human receptor-type tyrosine kinase gene (flt) closely related to the fms family. *Oncogene* **5**, 519–524 (1990).
12. C. de Vries *et al*., The fms-like tyrosine kinase, a receptor for vascular endothelial growth factor. *Science* **255**, 989–991 (1992).
13. B. I. Terman *et al*., Identification of the KDR tyrosine kinase as a receptor for vascular endothelial cell growth factor. *Biochem. Biophys. Res. Commun.* **187**, 1579–1586 (1992).
14. V. Joukov *et al*., A novel vascular endothelial growth factor, VEGF-C, is a ligand for the Flt4 (VEGFR-3) and KDR (VEGFR-2) receptor tyrosine kinases. *EMBO J.* **15**, 290–298 (1996).
15. K. Alitalo, T. Tammela, T. V. Petrova, Lymphangiogenesis in development and human disease. *Nature* **438**, 946–953 (2005).
16. A. K. Olsson, A. Dimberg, J. Kreuger, L. Claesson-Welsh, VEGF receptor signalling - in control of vascular function. *Nat. Rev. Mol. Cell Biol.* **7**, 359–371 (2006).
17. N. Ferrara, VEGF and the quest for tumour angiogenesis factors. *Nat. Rev. Cancer* **2**, 795–803 (2002).
18. J. W. Miller, J. Le Couter, E. C. Strauss, N. Ferrara, Vascular endothelial growth factor a in intraocular vascular disease. *Ophthalmology* **120**, 106–114 (2013).
19. L. G. Presta *et al*., Humanization of an anti-vascular endothelial growth factor monoclonal antibody for the therapy of solid tumors and other disorders. *Cancer Res.* **57**, 4593–4599 (1997).
20. Y. Chen *et al*., Selection and analysis of an optimized anti-VEGF antibody: Crystal structure of an affinity-matured Fab in complex with antigen. *J. Mol. Biol.* **293**, 865–881 (1999).
21. S. M. Chamow, T. Ryll, H. B. Lowman, D. Farson, Eds., *Therapeutic Fc-Fusion Proteins* (Wiley Blackwell, 2014).
22. J. Holash *et al*., VEGF-trap: A VEGF blocker with potent antitumor effects. *Proc. Natl. Acad. Sci. U.S.A.* **99**, 11393–11398 (2002).
23. M. G. Maguire *et al*.; Comparison of Age-related Macular Degeneration Treatments Trials (CATT) Research Group, Five-year outcomes with anti-vascular endothelial growth factor treatment of neovascular age-related macular degeneration: The comparison of age-related macular degeneration treatments trials. *Ophthalmology* **123**, 1751–1761 (2016).
24. F. G. Holz *et al*., Multi-country real-life experience of anti-vascular endothelial growth factor therapy for wet age-related macular degeneration. *Br. J. Ophthalmol.* **99**, 220–226 (2015).
25. J. T. Regula *et al*., Targeting key angiogenic pathways with a bispecific CrossMAb optimized for neovascular eye diseases. *EMBO Mol. Med.* **8**, 1265–1288 (2016).
26. G. A. Rodrigues *et al*., Functional characterization of abicipar-pegol, an anti-VEGF DARPin therapeutic that potently inhibits angiogenesis and vascular permeability. *Invest. Ophthalmol. Vis. Sci.* **59**, 5836–5846 (2018).
27. H. Vorum, T. K. Olesen, J. Zinck, M. Størling Hedegaard, Real world evidence of use of anti-VEGF therapy in Denmark. *Curr. Med. Res. Opin.* **32**, 1943–1950 (2016).
28. F. G. Holz *et al*., Single-chain antibody fragment VEGF inhibitor RTH258 for neovascular age-related macular degeneration: A randomized controlled study. *Ophthalmology* **123**, 1080–1089 (2016).
29. C. R. Baumal *et al*., Retinal vasculitis and intraocular inflammation after intravitreal injection of brolucizumab. *Ophthalmology* **127**, 1345–1359 (2020).
30. P. A. Campochiaro *et al*., The port delivery system with ranibizumab for neovascular age-related macular degeneration: Results from the randomized phase 2 ladder clinical trial. *Ophthalmology* **126**, 1141–1154 (2019).
31. T. Davis-Smyth, H. Chen, J. Park, L. G. Presta, N. Ferrara, The second immunoglobulin-like domain of the VEGF tyrosine kinase receptor Flt-1 determines ligand binding and may initiate a signal transduction cascade. *EMBO J.* **15**, 4919–4927 (1996).
32. C. Wiesmann *et al*., Crystal structure at 1.7 A resolution of VEGF in complex with domain 2 of the Flt-1 receptor. *Cell* **91**, 695–704 (1997).
33. H. W. Christinger, G. Fuh, A. M. de Vos, C. Wiesmann, The crystal structure of placental growth factor in complex with domain 2 of vascular endothelial growth factor receptor-1. *J. Biol. Chem.* **279**, 10382–10388 (2004).
34. S. Markovic-Mueller *et al*., Structure of the full-length VEGFR-1 extracellular domain in complex with VEGF-A. *Structure* **25**, 341–352 (2017).
35. N. Ferrara *et al*., Vascular endothelial growth factor is essential for corpus luteum angiogenesis. *Nat. Med.* **4**, 336–340 (1998).
36. H. P. Gerber *et al*., VEGF couples hypertrophic cartilage remodeling, ossification and angiogenesis during endochondral bone formation. *Nat. Med.* **5**, 623–628 (1999).
37. H. P. Gerber *et al*., VEGF is required for growth and survival in neonatal mice. *Development* **126**, 1149–1159 (1999).
38. H. P. Gerber, J. Kowalski, D. Sherman, D. A. Eberhard, N. Ferrara, Complete inhibition of rhabdomyosarcoma xenograft growth and neovascularization requires blockade of both tumor and host vascular endothelial growth factor. *Cancer Res.* **60**, 6253–6258 (2000).
39. I. F. Lissbrant *et al*., Neutralizing VEGF bioactivity with a soluble chimeric VEGF-receptor protein flt(1-3)IgG inhibits testosterone-stimulated prostate growth in castrated mice. *Prostate* **58**, 57–65 (2004).
40. M. Zheng, S. Deshpande, S. Lee, N. Ferrara, B. T. Rouse, Contribution of vascular endothelial growth factor in the neovascularization process during the pathogenesis of herpetic stromal keratitis. *J. Virol.* **75**, 9828–9835 (2001).
41. E. S. Kim *et al*., Potent VEGF blockade causes regression of coopted vessels in a model of neuroblastoma. *Proc. Natl. Acad. Sci. U.S.A.* **99**, 11399–11404 (2002).
42. K. A. Houck, D. W. Leung, A. M. Rowland, J. Winer, N. Ferrara, Dual regulation of vascular endothelial growth factor bioavailability by genetic and proteolytic mechanisms. *J. Biol. Chem.* **267**, 26031–26037 (1992).
43. P. Malyala, M. Singh, Endotoxin limits in formulations for preclinical research. *J. Pharm. Sci.* **97**, 2041–2044 (2008).
44. M. Shibuya, VEGFR and type-V RTK activation and signaling. *Cold Spring Harb. Perspect. Biol.* **5**, a009092 (2013).
45. J. E. Park, H. H. Chen, J. Winer, K. A. Houck, N. Ferrara, Placenta growth factor. Potentiation of vascular endothelial growth factor bioactivity, in vitro and in vivo, and high affinity binding to Flt-1 but not to Flk-1/KDR. *J. Biol. Chem.* **269**, 25646–25654 (1994).
46. M. S. Brozzo *et al*., Thermodynamic and structural description of allosterically regulated VEGFR-2 dimerization. *Blood* **119**, 1781–1788 (2012).

47. N. Kwak, N. Okamoto, J. M. Wood, P. A. Campochiaro, VEGF is major stimulator in model of choroidal neovascularization. *Invest. Ophthalmol. Vis. Sci.* **41**, 3158–3164 (2000).
48. Y. Saishin *et al*., VEGF-TRAP(R1R2) suppresses choroidal neovascularization and VEGF-induced breakdown of the blood-retinal barrier. *J. Cell. Physiol.* **195**, 241–248 (2003).
49. C. Campa *et al*., Effects of an anti-VEGF-A monoclonal antibody on laser-induced choroidal neovascularization in mice: Optimizing methods to quantify vascular changes. *Invest. Ophthalmol. Vis. Sci.* **49**, 1178–1183 (2008).
50. S. Bogdanovich *et al*., Human IgG1 antibodies suppress angiogenesis in a target-independent manner. *Signal Transduct. Target. Ther.* **1**, 15001 (2016).
51. R. L. E. Silva *et al*., Tyrosine kinase blocking collagen IV-derived peptide suppresses ocular neovascularization and vascular leakage. *Sci. Transl. Med.* **9**, eaai8030 (2017).
52. J. E. Lee *et al*., Novel glycosylated VEGF decoy receptor fusion protein, VEGF-Grab, efficiently suppresses tumor angiogenesis and progression. *Mol. Cancer Ther.* **14**, 470–479 (2015).
53. M. Park, S. T. Lee, The fourth immunoglobulin-like loop in the extracellular domain of FLT-1, a VEGF receptor, includes a major heparin-binding site. *Biochem. Biophys. Res. Commun.* **264**, 730–734 (1999).
54. H. Gerhardt *et al*., VEGF guides angiogenic sprouting utilizing endothelial tip cell filopodia. *J. Cell Biol.* **161**, 1163–1177 (2003).
55. H. F. Dvorak *et al*., Distribution of vascular permeability factor (vascular endothelial growth factor) in tumors: Concentration in tumor blood vessels. *J. Exp. Med.* **174**, 1275–1278 (1991).
56. K. H. Plate, G. Breier, H. A. Weich, W. Risau, Vascular endothelial growth factor is a potential tumour angiogenesis factor in human gliomas in vivo. *Nature* **359**, 845–848 (1992).
57. Qu-Hong, J. A. Nagy, D. R. Senger, H. F. Dvorak, A. M. Dvorak, Ultrastructural localization of vascular permeability factor/vascular endothelial growth factor (VPF/VEGF) to the abluminal plasma membrane and vesiculovacuolar organelles of tumor microvascular endothelium. *J. Histochem. Cytochem*. **43**, 381–389 (1995).
58. D. Yang, A. Singh, H. Wu, R. Kroe-Barrett, Comparison of biosensor platforms in the evaluation of high affinity antibody-antigen binding kinetics. *Anal. Biochem.* **508**, 78–96 (2016).
59. J. Yang *et al*., Comparison of binding characteristics and in vitro activities of three inhibitors of vascular endothelial growth factor A. *Mol. Pharm.* **11**, 3421–3430 (2014).
60. H. P. Gerber *et al*., Mice expressing a humanized form of VEGF-A may provide insights into the safety and efficacy of anti-VEGF antibodies. *Proc. Natl. Acad. Sci. U.S.A.* **104**, 3478–3483 (2007).
61. M. F. Bachmann *et al*., The role of antibody concentration and avidity in antiviral protection. *Science* **276**, 2024–2027 (1997).
62. Y. Ichiyama *et al*., The systemic antiangiogenic effect of intravitreal aflibercept injection in a mouse model of retinopathy of prematurity. *FASEB J.* **35**, e21390 (2021).
63. M. M. Le Goff, P. N. Bishop, Adult vitreous structure and postnatal changes. *Eye (Lond.)* **22**, 1214–1222 (2008).
64. J. Morin *et al*.; Canadian Neonatal Network and the Canadian Neonatal Follow-Up Network Investigators, Neurodevelopmental outcomes following bevacizumab injections for retinopathy of prematurity. *Pediatrics* **137**, e20153218 (2016).
65. M. J. Sankar, J. Sankar, P. Chandra, Anti-vascular endothelial growth factor (VEGF) drugs for treatment of retinopathy of prematurity. *Cochrane Database Syst. Rev.* **1**, CD009734 (2018).
66. B. Barleon *et al*., Mapping of the sites for ligand binding and receptor dimerization at the extracellular domain of the vascular endothelial growth factor receptor FLT-1. *J. Biol. Chem.* **272**, 10382–10388 (1997).
67. C. J. Roberts, Therapeutic protein aggregation: Mechanisms, design, and control. *Trends Biotechnol.* **32**, 372–380 (2014).
68. K. D. Ratanji, J. P. Derrick, R. J. Dearman, I. Kimber, Immunogenicity of therapeutic proteins: Influence of aggregation. *J. Immunotoxicol.* **11**, 99–109 (2014).
69. L. Yu *et al*., Interaction between bevacizumab and murine VEGF-A: A reassessment. *Invest. Ophthalmol. Vis. Sci.* **49**, 522–527 (2008).
70. H. Xin, C. Zhong, E. Nudleman, N. Ferrara, Evidence for pro-angiogenic functions of VEGF-ax. *Cell* **167**, 275–284.e6 (2016).
71. C. Zhong *et al*., Inhibition of protein glycosylation is a novel pro-angiogenic strategy that acts via activation of stress pathways. *Nat. Commun.* **11**, 6330 (2020).
72. S. Xiao *et al*., Fully automated, deep learning segmentation of oxygen-induced retinopathy images. *JCI Insight* **2**, e97585 (2017).